Protein phosphatases maintain the organization and structural interactions of hepatic keratin intermediate filaments

Diana M. Toivola[1,4], Robert D. Goldman[2], David R. Garrod[3] and John E. Eriksson[4,*]

[1]Department of Biology, Åbo Akademi University, BioCity, Artillerig. 6, FIN-20520 Turku, Finland
[2]Department of Cell and Molecular Biology, Northwestern University Medical School, 303 East Chicago Avenue, Chicago, IL 60611-3008, USA
[3]School of Biological Sciences, University of Manchester, 3.239 Stopford Building, Oxford Road, Manchester, M13 9PT, UK
[4]Turku Centre for Biotechnology, BioCity, POB 123, FIN-20521, Turku, Finland

*Author for correspondence (e-mail: jeriksso@mail.abo.fi)

SUMMARY

The importance of protein phosphatases in the maintenance of cytoskeletal structure is supported by the serious liver injury caused by microcystin-LR, a hepatotoxic inhibitor of type-1 and type-2A serine/threonine protein phosphatases. We used the microcystin-LR-induced cell injury as a model to study the roles of protein dephosphorylation in maintaining cytoskeletal structure and cellular interactions in primary rat hepatocyte cultures. Confocal microscopy revealed that the first visible effect of microcystin-LR is disruption of desmoplakin organization at the cell surface, indicating dissociation of desmosomes. This effect is followed by a dramatic reorganization of both the intermediate filament (keratins 8 and 18) and microfilament networks, resulting in a merged structure in which the intermediate filaments are organized around a condensed actin core. Keratin 8, keratin 18 and desmoplakin I/II are the major cytoskeleton-associated targets for microcystin-LR-induced phosphorylation. Hyperphosphorylation of keratin 8 and 18 is accompanied by an increased keratin solubility, which correlates with the observed morphological effects. Phosphopeptide mapping shows that four specific tryptic phosphopeptides are highly phosphorylated predominantly in the soluble pool of keratin 18, whereas keratin 8 shows no indications of such assembly state-specific sites. Phosphopeptide maps of keratins phosphorylated in vivo and in vitro indicate that Ca^{2+}/calmodulin-dependent kinase may be involved in regulating the serine-specific phosphorylation of both keratin 8 and keratin 18, while cAMP-dependent protein kinase does not seem to play a major role in this context. Taken together, our results show that the interactions between keratin intermediate filaments and desmosomes as well as the assembly states of their main constituent proteins, are directly regulated by serine/threonine kinase/phosphatase equilibria.

Key words: Protein phosphorylation, Microcystin-LR, Microfilament, Intermediate filament, Keratin, Desmosome, Desmoplakin, Ca^{2+}/calmodulin-dependent protein kinase, cAMP-dependent protein kinase

INTRODUCTION

Protein phosphorylation has been established as a principal mechanism in the regulation of cytoskeletal structure and organization. Phosphorylation controls the cytoskeleton at specific key events during the cell cycle and during cell differentiation, and is also involved in the regulation of steady-state homeostasis of many cytoskeletal proteins. In this regard, serine/threonine(ser/thr)-specific protein phosphatases are of crucial importance in maintaining cytoskeletal integrity (Eriksson et al., 1990a, 1992a,b). The remarkable liver damage induced by the liver-specific phosphatase inhibitor microcystin-LR (MC-LR) illustrates well the essential nature of this constitutive phosphatase activity. MC-LR belongs to a group of cyclic hepatotoxic peptides called microcystins which bind to (Toivola et al., 1994; MacKintosh et al., 1995) and inhibit type-1 (PP1) and type-2A (PP2A) ser/thr protein phosphatases (reviewed by Fujiki and Suganuma, 1993; Holmes and Boland, 1993). At tissue level, microcystins induce extensive hepatic hemorrhage with a complete disruption of the lobular and sinusoidal liver architecture, leading to rapid death by hemodynamic shock (Falconer et al., 1981; Eriksson et al., 1988; Hooser et al., 1989). This liver disruption appears to be a consequence of a marked and rapid cytoskeletal reorganization in the parenchymal cells (Eriksson et al., 1989; Falconer and Yeung, 1992; Wickstrom et al., 1995). The liver-targeted effects of microcystins are due to selective uptake (Meriluoto et al., 1990) through a hepatocyte-specific organic anion carrier system, the multispecific bile acid transport system (Eriksson et al., 1990b; Runnegar et al., 1991). The specific and targeted action of microcystins make them highly useful as biochemical probes for elucidating the roles of ser/thr protein phosphatases in maintaining cytoskeletal organization of hepatocytes as well as structural integrity of the liver parenchyma.

Other well characterized ser/thr protein phosphatase inhibitors, such as okadaic acid and calyculin A, have similar inhibitory potencies as microcystins but are freely membrane-permeable (for reviews see Fujiki and Suganuma, 1993;

Holmes and Boland, 1993). By analogy with the effects of microcystins in hepatocytes, these compounds cause severe and rapid alterations of cytoskeletal structure in various cell models, representing many of the basic cell types in mammalian tissues (reviewed by Eriksson and Goldman, 1993; see also Hirano et al., 1992; Kreinbühl et al., 1992; Almazan et al., 1993; Deery, 1993; Downey et al., 1993; Hosoya et al., 1993; Kasahara et al., 1993; Kurisaki et al., 1993; Yano et al., 1995; Maier et al., 1995; Wickstrom et al., 1995). The inhibitor-induced cytoskeletal effects are reversible at low concentrations (Eriksson et al., 1992a) and, therefore, these effects reflect specific phosphorylation-dependent regulatory mechanisms rather than unspecific changes in cellular homeostasis (Eriksson and Goldman, 1993). As protein phosphatase inhibitors alter cytoskeletal organization regardless of the cell type, it seems evident that there is a general requirement for high constitutive protein phosphatase activities to maintain cytoskeletal integrity in interphase cells. One striking feature of many of these studies has been the rapid loss of cell type-specific intermediate filament (IF) structures as a consequence of rapid phosphorylation of the constituent IF proteins (Eriksson et al., 1992a,b; Lee et al., 1992; Deery, 1993; Almazan et al., 1993). There is now substantial evidence that the dynamics and polymerization states of IFs are directly regulated by protein phosphorylation/dephosphorylation (for reviews see Eriksson et al., 1992b; Eriksson and Goldman, 1993; Heins and Aebi, 1994). This implies that these structures, generally regarded as very stable and static, are significantly more dynamic than previously assumed. With respect to microcystins, a previous study has indicated that MC-LR induces hyperphosphorylation of the major IF proteins in hepatocytes, keratin 8 (K8) and keratin 18 (K18; Ohta et al., 1992). The phosphorylation of specific sites of human K8 and K18 IFs seems to be critical for the filament assembly dynamics (Ku and Omary, 1994) and is likely to play a role in the functions of these keratins (Liao et al., 1995).

In the present study, we have used MC-LR to elucidate the roles of protein phosphatases and dephosphorylation in maintaining the integrity of the hepatocyte keratin IF cytoskeleton, as well as desmosomal interactions between hepatocytes. Keratin filaments in epithelial cells are attached to desmosomes via the desmosomal phosphoproteins desmoplakin I and II (DPI/DPII; reviewed by Garrod, 1993), and DPI/DPII are, thus, potentially affected by MC-LR. Our study reveals that the structure of keratin IFs, as well as their interactions with desmosomes, is directly dependent on ser/thr protein phosphatase activity. We focused on clarifying the detailed mechanisms underlying the phosphorylation-dependent disruption of these cellular structures. MC-LR-induced cell injury is known to involve a remarkable reorganization of microfilaments (MF) in hepatocytes (Eriksson et al., 1989; Runnegar and Falconer, 1986; Falconer and Yeung, 1992; Wikstrom et al., 1995). In relation to this, our study also reveals an interesting interaction between IFs and MFs.

MATERIALS AND METHODS

Chemicals and antibodies

MC-LR was isolated and purified from the blue green alga *Microcystis aeruginosa* as described earlier (Meriluoto and Eriksson, 1988) and calyculin A was purchased from Moana BioProducts, Inc. (Honolulu, HI, USA). Tetramethylrhodamine (TRITC)-conjugated phalloidin (P-5157, Sigma Chemical Company, St Louis, MO, USA) was used to localize F-actin. Polyclonal antibodies against K8 and K18 were produced in rabbits using the keratins from a rat liver IF preparation (see below) as immunogens. The liver keratins were separated on 10% SDS-PAGE, and the keratin bands were electroeluted after excision from a Coomassie-stained gel. Rabbits were immunized with 0.5 mg keratins in Freund's complete adjuvant. Tissue sample testing by immunoblotting and immunofluorescence labeling of frozen-sectioned tissue showed that the antibodies reacted only with K8 and K18 in simple epithelia. The mouse monoclonal antibody used for immunostaining of desmoplakin was characterized as previously described (Parrish et al., 1987). The rabbit polyclonal anti-desmoplakin antibody used for immunoprecipitations was raised to gel-purified bovine desmosomal proteins and characterized according to the protocol of Cowin and Garrod (1983). Myosin light chain was studied using the monoclonal anti-myosin antibody (light chains 20K), clone MY-21 mouse ascites fluid (M-4401, Sigma). Secondary antibodies used for fluorescence microscopy were fluorescein (FITC)-conjugated rabbit anti-mouse immunoglobulins (F313, Dakopatt, Glostrup, Denmark), FITC-conjugated swine anti-rabbit immunoglobulins (F205, Dakopatt) and TRITC-conjugated goat anti-rabbit immunoglobulins (Molecular Probes, Eugene, OR, USA). Secondary antibodies used for immunoblotting were peroxidase-labeled sheep anti-mouse immunoglobulins (NA 931, Amersham, Buckinghamshire, UK) and peroxidase-labeled donkey or goat anti-rabbit immunoglobulins (NIF 824, Amersham and W401B, Promega, Madison, WI, USA, respectively). Chemicals were of highest purity grade and, if not otherwise stated, purchased from Sigma or Merck (Darmstadt, Germany). Radiochemicals were from Amersham or ICN (Costa Mesa, CA, USA).

Liver cells and microscopy

Hepatocytes were isolated from male Wistar rats (200-250 g) by a two-step collagenase perfusion of the liver as described by Seglen (1976). For suspension cultures, cells were incubated in the original 'suspension buffer' (Seglen, 1976) at $1-2\times10^6$ cells/ml, 37°C in a shaking bath. Primary hepatocyte cultures were prepared as follows: after perfusion of the liver with collagenase buffer, cells were dissociated in sterile DMEM (Dulbecco's modified Eagle's medium), filtered through 100 μm and 75 μm mesh filters, and washed once in DMEM. Cells were plated on collagen-coated (6 μg/cm²) cover slips or tissue culture dishes at a density of $5-20\times10^4$ cells/ml in Williams' medium E (W-4125, Sigma) supplemented with 10% fetal calf serum, gentamycin (50 μg/ml) and an ITSS-mixture containing insulin (5 μg/ml), transferrin (5 μg/ml) and sodium selenite (0.005 μg/ml). After 1-2 hours the settled cells were washed once in DMEM and the medium was changed to fresh Williams' medium E supplemented with gentamycin, ITSS, dexamethasone (100 nM), glucagon (1 nM), linoleic acid (5 μg/ml in BSA; final BSA concentration 500 μg/ml) and allowed to grow overnight. Prior to the experiments, the medium was replaced with fresh medium. Cultures were used within 36 hours after plating.

Cells were grown on coverslips for indirect immunofluorescence observations of cytoskeletal proteins. Cells were washed in PBS and fixed in dehydrated −20°C methanol for 10 minutes (for double-staining of K8/K18 and desmoplakin) or in 1% paraformaldehyde for 20 minutes at room temperature (RT) (for double-staining of F-actin and K8/K18). Cells were washed in PBS, blocked with 1% BSA and incubated with the respective primary antibodies in 1% BSA for 60 minutes at RT. Cells were further washed with PBS, incubated with the secondary antibody in 1% BSA and finally washed before mounting in Mowiol 40-88 (32, 459-0, Aldrich-Chemie, Steinheim, Germany) supplemented with 100 mg/ml 1,4,diazabicyclo[2.2.2]-octane (D 2,780-2, Aldrich-Chemie). Cells double-stained for F-actin and K8/K18 were prior to blocking permeabilized with 0.2%

Nonident P-40 (NP-40). Samples were analyzed in a Leitz Aristoplan fluorescence microscope and a Leica TCS40 confocal laser scanning microscope using the program SCANware 4.2a. Primary cultured hepatocytes were grown and processed for transmission electron microscopy (TEM) in 24-well culture dishes (Eriksson et al., 1989).

Identification of phosphoproteins

Primary cultured hepatocytes were metabolically labeled with 100-200 µCi/ml [^{32}P]orthophosphate for 2 hours in Williams' medium E (suspension cultures: 300 µCi/ml [^{32}P]orthophosphate, 1.5 hours). This was found to be sufficient to saturate the ATP pools with ^{32}P, prior to addition of MC-LR. After labeling and treatment, the incubation medium was removed and the adherent cells were washed once with ice-cold PBS. The incubation medium was centrifuged (1,000 *g*, 2 minutes) and the pellet further washed with PBS, to collect any detached cells. Nonradioactive samples for immunoblotting analyses were treated as above, excluding the [^{32}P]orthophosphate incubation. All results presented represent data collected from a minimum of 3 experiments.

Whole cell extracts

These were obtained by lysing cells in SDS-buffer (20 mM Tris-HCl, pH 7.2, 5 mM EGTA, 5 mM EDTA, 0.4% SDS, 10 mM sodium pyrophosphate, 1 mM PMSF, 10 µg/ml antipain, 10 µg/ml leupeptin). Cells were detached from the culture dish with a cell scraper, boiled for 5-10 minutes, and sonicated for 20 seconds with a probe sonicator.

Separation of Triton X-100 (TX-100) soluble and insoluble fractions

TX-100 buffer (20 mM Hepes, pH 7.6, 100 mM NaCl, 5 mM MgCl$_2$, 5 mM EGTA, 1% TX-100, 1 mM PMSF, 10 µg/ml leupeptin, 10 µg/ml antipain) was added to culture dishes, cells were detached and collected, homogenized on ice (20 strokes in a 5 ml homogenizer) and centrifuged for 15 minutes at 15,000 *g* (4°C) to obtain the TX-100 soluble (supernatant) and insoluble (pellet) fractions. Both fractions were dissolved either in 3× Laemmli sample buffer (Laemmli, 1970) or in urea buffer (9.5 M urea, 2% NP-40, 5% 2-mercaptoethanol, 2% ampholines – 1 part of ampholines 5/7, and 4 parts of 3/10; Pharmacia, Sweden) for further 1- or 2-dimensional (2-D) gel electrophoretic separation, respectively.

K8/K18 were co-immunoprecipitated by dilution of whole cell extracts with RIP-buffer (20 mM Hepes, pH 7.4, 140 mM NaCl, 10 mM pyrophosphate, 5 mM EDTA, 0.4% NP-40, 1 mM PMSF, 10 µg/ml leupeptin, 10 µg/ml antipain) added to a 1+1 mixture of the polyclonal rabbit anti-K8 and -K18 antibodies, and finally recovered with Protein A-Sepharose (Ottaviano and Gerace, 1985). Desmoplakins were immunoprecipitated with the polyclonal anti-desmoplakin antibody using the same method. Proteins and cell extracts were separated on SDS-polyacrylamide gels (SDS-PAGE; Laemmli, 1970) and/or 2-D polyacrylamide gel electrophoresis (2-D PAGE; O'Farrell, 1975). Gels were stained with either Coomassie brilliant blue or silver staining to control for equal loading of proteins, dried and autoradiographed at −70°C using Kodak X-Omat AR, Kodak Biomax MR or MS films. Specific ^{32}P-labeling of proteins was quantified using a phosphorimage analyzer (Bio-Rad GS-250 Molecular Imager or Fuji BAS 1000). For immunoblotting, proteins were electrotransferred from gels to nitrocellulose membranes. Binding of primary antibody to the proteins was detected using horseradish peroxidase-labeled secondary antibodies and the ECL western blotting detection system (Amersham).

For phosphopeptide mapping or phosphoamino acid analysis immunoprecipitated K8/K18, or TX-100 fractions, were separated on 10% SDS-PAGE, fixed in 50% methanol, dried and exposed to film. The phosphorylated keratin bands K8 (55 kDa) and K18 (49 kDa) were cut out from gels and digested twice (9 + 3 hours) in trypsin (T-8642, Sigma; 10 µg/ml in 50 mM ammonium bicarbonate) at 37°C. The digested peptides were washed with double distilled water and dried using a Speed vac. Peptide maps of the trypsin-digested keratin samples (van der Geer et al., 1993) were obtained by 2-D separation on microcristalline cellulose thin layer chromatography (TLC)-plates (13660087, Eastman Kodak Company, Rochester, NY, USA). Trypsinized keratin peptides were also subjected to phosphoamino acid analysis by acid hydrolysis and further 2-D TLC electrophoresis together with P-Ser, P-Tyr, and P-Thr standards (van der Geer et al., 1993). Phosphoamino acids were visualized with ninhydrin staining and autoradiography (van der Geer et al., 1993).

In vitro phosphorylation of rat keratins

For liver keratin isolation, livers from Wistar rats were minced and homogenized in a Potter-Elvehjelm homogenizer on ice in a buffer (0.6 M KCl, 2 mM MgCl$_2$, 5 mM EGTA, 1% TX-100, 1 mM PMSF, 10 µg/ml leupeptin and 10 µg/ml antipain in PBS, pH 7.6, 10 ml/liver), and centrifuged at 10,000 *g* for 10 minutes at 4°C. Pellets were washed 3× with PBS supplemented with 5 mM EGTA and 1 mM PMSF by centrifugation as above. Pellets were sonicated on ice in 8 M urea, 10 mM Hepes, pH 7.2, 0.2% 2-mercaptoethanol and 1 mM PMSF (1-2 ml/liver) and further centrifuged at 200,000 *g* for 45 minutes at 20°C. The supernatant was dialyzed twice (2-3 hours, 4°C) in 10 mM Hepes, pH 7.2, 0.2% 2-mercaptoethanol and 0.2 mM PMSF. The resulting keratin IF preparations were stored at −20°C.

Keratins (0.05-0.1 mg) were phosphorylated with ATP (20 µM ATP, A-5394, Sigma, and 10 µCi [^{32}P]ATP) using 1 µg of the activated catalytic subunit (P-2645, Sigma) of cAMP-dependent protein kinase (PKA). The kinase reaction was carried out in 10 mM Hepes, pH 7.2, 60 mM NaCl, 0.5 mM CaCl$_2$, 2.5 mM EGTA and 2 mM MgCl$_2$ at 37°C, and stopped after 30 minutes by addition of 1 volume of 3× Laemmli sample buffer (Laemmli, 1970). Keratins were also phosphorylated in vitro using CaMK (Ca^{2+}/calmodulin- dependent kinase; a kind gift from Prof. H. Schulman, Dept of Neurobiology, Stanford University School of Medicine, Stanford, CA). The kinase reaction-mixture contained keratins (0.05-0.1 mg), 0.5 mM CaCl$_2$, 60 U/100 µl calmodulin (P-1915, Sigma) and ATP (40 µM ATP + 10 µCi [^{32}P]ATP) in a buffer with 50 mM Pipes, pH 7.0, 10 mM MgCl$_2$ and 0.2 mM EGTA. The reaction was carried out for 15 minutes at 30°C and stopped with 3× Laemmli sample buffer. The in vitro phosphorylated keratins were separated by SDS-PAGE, autoradiographed, cut out from the gel, digested with trypsin and further separated by 2-D TLC phosphopeptide mapping as described above.

RESULTS

Desmoplakin organization is altered at an early stage of ser/thr protein phosphatase inhibition

As there is evidence to show that the interaction between keratin IFs and desmosomal plaque proteins is regulated by phosphorylation (Stappenbeck et al., 1994; Pasdar et al., 1995), we wanted to determine how the MC-LR-induced phosphatase inhibition affects desmosomal integrity in liver cells. Impaired desmosomal functions could partly explain the MC-LR-induced organ damage. To assess desmosomal structure we observed the immunofluorescence staining pattern of desmoplakin. In primary cultures of rat hepatocytes, desmoplakin was seen as spots or discontinuous bands in areas of cell-cell contacts (Fig. 1A). In these regions, the staining pattern was closely associated with K8/K18 immunostaining (Fig. 1A,D), which elsewhere in the cell was seen as a delicate filament network, extending from the perinuclear region to the most peripheral parts of the cell (Fig. 1D, see also Fig. 2A,G). The desmoplakin pattern was clearly altered at 12 minutes of MC-LR-exposure, before any major
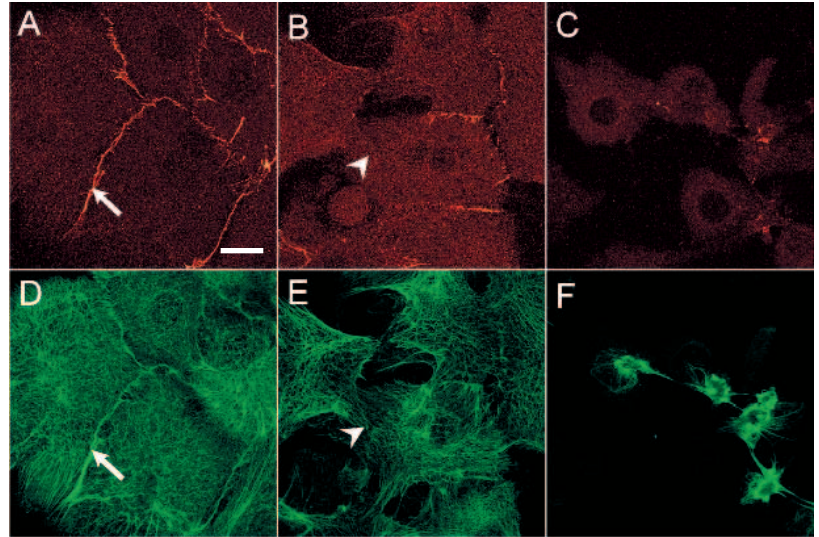
Fig. 1. The effects of MC-LR on desmosomal structure. Immunolocalization of desmoplakin (red) and K8/K18 (green) in double-stained primary cultured rat hepatocytes is showing control cells (A and D) and cells treated with 4 μM MC-LR for 12 minutes (B and E) and 22 minutes (C and F). Pictures are maximal projections of 12 confocal laser scanning images taken with 0.3-0.5 μm intervals through the cells and projected on 2 dimensions. Bar is 10 μm. Arrows show desmoplakin and keratin colocalization and arrowheads regions of lost desmoplakin staining. In these regions, obvious keratin IF withdrawal is seen.
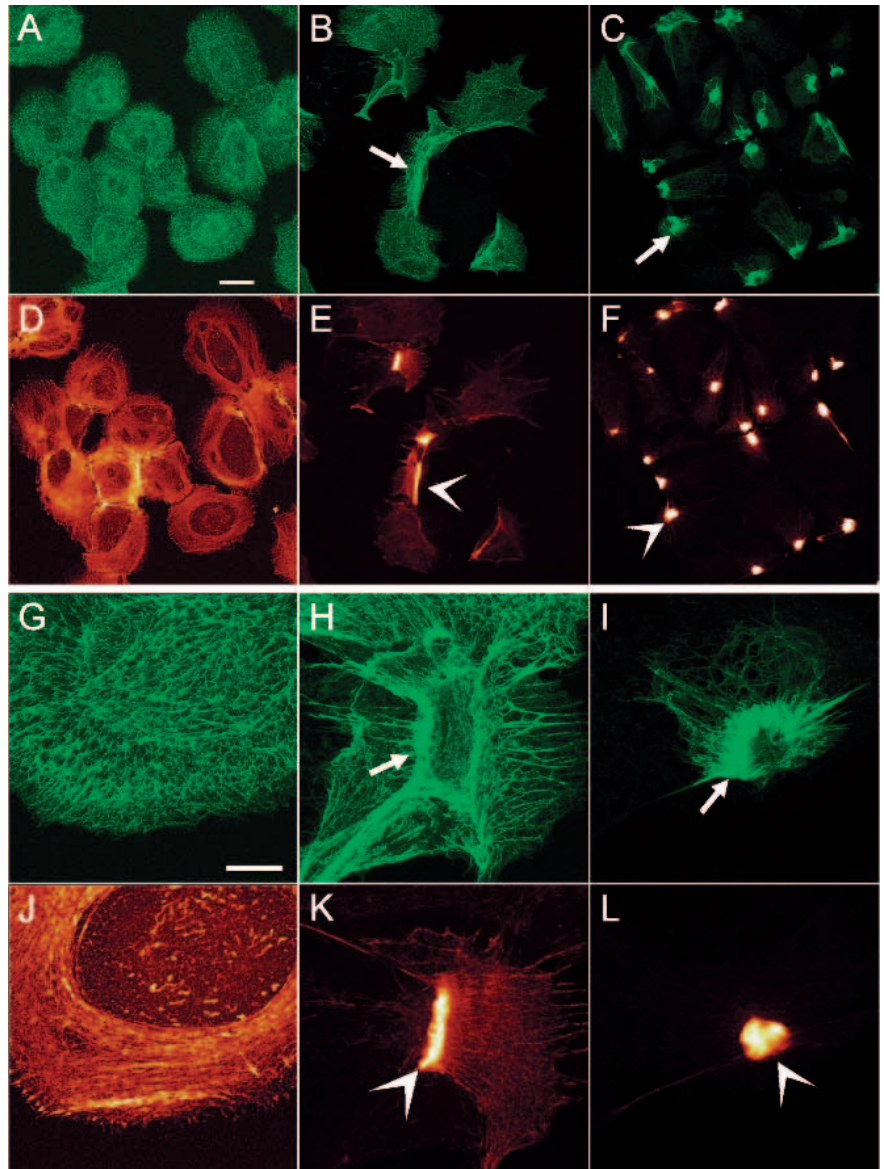

Fig. 2. Reorganization of IFs and MFs in primary hepatocyte cultures treated with MC-LR. The confocal micrographs show immunolocalization of IFs (K8/K18, green: A-C and G-I) and MFs (F-actin, red: D-F and J-L) in double-stained primary hepatocyte control cells (A,D,G,J), cells treated with 4 μM MC-LR for 15 minutes (B,E,H,K) and 30 minutes (C,F,I,L). Double-stained cells in G-L show a higher magnification of one of the cells in A-F. Pictures are maximal projections of 12 confocal images taken with 0.3-0.5 μm intervals through the cell and projected on 2 dimensions. Bar in A (for A-F) is 30 μm and in G (for G-L) 10 μm. The condensed K8/K18 and F-actin are indicated with arrows and arrowheads, respectively.

effects could be seen in the distribution of keratin IFs (Fig. 1B,E). The desmoplakin immunoreactivity was greatly decreased at the locations of lost cell contacts (Fig. 1B), indicating dissociation of cell junctions. An increased diffuse staining in the cell body (Fig. 1B) at this point suggests that desmoplakins are dissociated from the desmosomes. This increase was observed more prominently with a conventional epifluorescence microscope (results not shown). Although the IF networks at this stage remained largely intact, co-staining for K8/K18 showed that the keratin filaments were withdrawn from regions where cell-cell contacts and desmoplakin staining were lost (Fig. 1E). At 22 minutes the desmoplakin immunoreactivity at cell borders had disappeared (Fig. 1C) and at this point the network of IF tonofilaments was completely reorganized (Fig. 1C,F, see the following section for details; Fig. 2).

MC-LR-induced reorganization of IFs and MFs

As previous studies have shown that MC-LR-induced phosphatase inhibition causes severe effects on the organization of MFs (Eriksson et al., 1989), we wanted to determine how this reorganization occurs in relation to the keratin IFs. In control hepatocytes, the immunoreactivity specific for K8/K18 IF networks (Fig. 2A,G) showed no marked colocalization with the F-actin-specific fluorescence pattern (Fig. 2D,J), although there may be colocalization at some specific regions. As mentioned above, the first visible MC-LR-induced effect on IFs occurred as an immediate consequence of the disruption of desmosomal structure, and was seen as a retraction of the IF networks from the regions of cell junctions (Fig. 1B,E). At this stage, there were no obvious effects on the MFs (results not shown). After 15 minutes the IFs had retracted from the edges of most cells and the organization of MFs was clearly altered (Fig. 2B,E,H,K). Interestingly, the reorganization of IFs and MFs occurred in a concerted manner. The IFs were organized towards the condensing MFs that appeared to form a leading edge, pulling the IFs towards one pole of the cell. After 30 minutes the IFs and MFs were completely reorganized into a merged structure, in which the MFs formed a condensed spherical structure which was surrounded in one plane by a collar of bundled keratins (Fig. 2C,F,I,L and Fig. 3). Thus, there appeared to be a strong interaction between IFs and MFs, as the condensing MFs formed an 'organization center' for the IFs that in this region remained assembled after disassembly of a significant proportion of the constituent keratin protein polymers (see below). The fluorescence pattern in the hepatocytes also indicated a significant degree of IF disassembly, observed as an increased diffuse background staining using conventional epifluorescence microscope (results not shown). At higher concentrations for longer periods (10 μM MC-LR for 50 and 120 minutes; results not shown), a decreasing number of the keratin IFs were observed in the condensed form. The MC-LR-induced reorganization of IFs and MFs was confirmed at the ultrastructural level (results not shown). Taken together, our microscopic data showed that the formed actin structure is a slightly convex circular plaque structure, opening towards the center of the cell. The bundled keratins are located around and beneath this actin structure. As a consequence of the altered cytoskeletal and desmosomal structures, the hepatocytes lost contact with each other and obtained a somewhat rounded morphology.
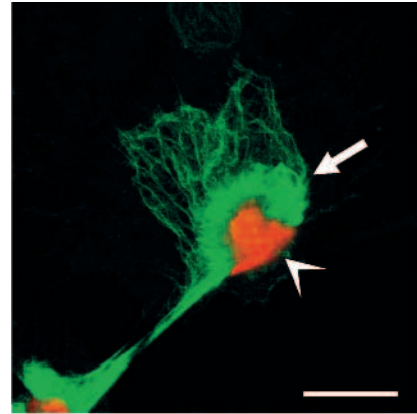

Fig. 3. Association of MFs and IFs in a MC-LR-treated hepatocyte. This high magnification confocal micrograph reveals the formed close association of MFs and keratin IFs in a double-stained primary hepatocyte treated with 4 μM MC-LR for 30 minutes. F-actin is shown in red (arrowhead) and K8/K18 immunofluorescence in green (arrow). The picture is a combination of 2 maximal projections of 12 confocal images each taken with 0.4 μm intervals throughout the cells and projected on 2 dimensions. Bar is 10 μm.

MC-LR induces hyperphosphorylation and disassembly of K8/K18 and DPI/DPII

To determine the protein phosphorylation states in the presence and absence of MC-LR, primary hepatocyte cultures were subjected to metabolic ^{32}P-labeling. MC-LR induced an overall increase in protein phosphorylation, as seen in cellular proteins separated into 1% TX-100 soluble and insoluble proteins (Fig. 4A, upper panel). Among the hyperphosphorylated proteins, two proteins with apparent molecular masses of 49 and 55 kDa were among the most extensively phosphorylated. Immunoprecipitates of K8/K18 from whole cell extracts confirmed that these proteins were K8 and K18 (Fig. 4B). The hyperphosphorylation of K8 and K18 was time- (Fig. 4A, upper panel, B) and concentration-dependent (results not shown). Measurements of the specific activities of K8 and K18 showed that MC-LR induced 1.1-fold (4 μM for 15 minutes), 8.7-fold (4 μM for 30 minutes), and 14.3-fold (10 μM for 50 minutes) increases in the ^{32}P-labeling of K8 immunoprecipitates (Fig. 4B). Corresponding increases in the relative ^{32}P-labeling of immunoprecipitated K18 were 5.3-, 69.0- and 78.0-fold higher than the K18 labeling in control cells (Fig. 4B). The MC-LR-induced phosphorylation of K18 increased somewhat prior to that of K8.

We further investigated whether the MC-LR-induced disassembly of K8/K18 could be related to phosphorylation-induced solubilization of keratins. This was studied by extracting cells with 1% TX-100, in which K8/K18 in interphase cells are primarily insoluble (Fig. 4A). While only trace amounts of K8 and K18 were found in the soluble fraction of control cells (Fig. 4A, lower panel), incubation with MC-LR induced a time-dependent solubilization or disassembly of keratin IFs, shown as an increased K8/K18 immunoreactivity on immunoblots of soluble extracts (Fig. 4A, lower panel). A corresponding decrease in the pool of insoluble keratins was seen, more markedly for K8 than K18 (Fig. 4A, lower panel). The time-dependent increase of solubilized K8/K18 (Fig. 4A, lower panel) corresponded well to the increase in phosphorylation of K8/K18
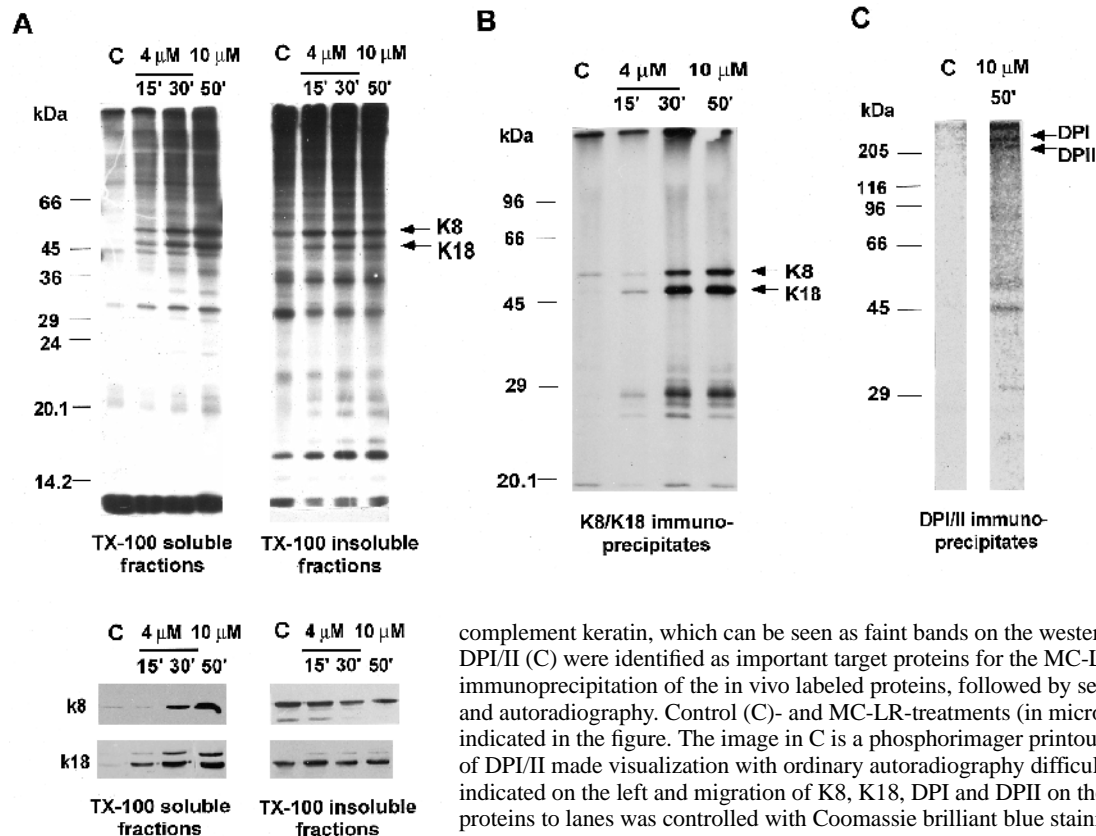
Fig. 4. Identification of hyperphosphorylated proteins in primary hepatocyte cultures treated with MC-LR. Autoradiographs show TX-100 soluble and insoluble fractions of ^{32}P-labeled proteins from primary cultured hepatocytes separated on 12.5% SDS-PAGE (A, upper panel). Immunoblots (10% SDS-PAGE) of TX-100 soluble and insoluble fractions with anti-K8 and -K18 antibodies (A, lower panel) show an increased solubility of both K8 and K18 upon MC-LR treatment. Both keratin antibodies showed a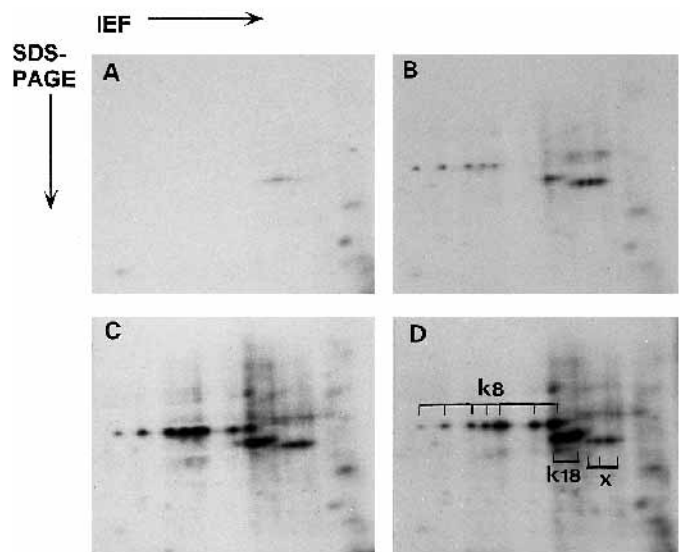 minor cross-reactivity with their complement keratin, which can be seen as faint bands on the western blots. K8/K18 (B) and DPI/II (C) were identified as important target proteins for the MC-LR-induced phosphorylation by immunoprecipitation of the in vivo labeled proteins, followed by separation on 10% SDS-PAGE and autoradiography. Control (C)- and MC-LR-treatments (in micromolar and minutes) are as indicated in the figure. The image in C is a phosphorimager printout, as the low labeling intensites of DPI/II made visualization with ordinary autoradiography difficult. Molecular masses (kDa) are indicated on the left and migration of K8, K18, DPI and DPII on the right. Equal loading of proteins to lanes was controlled with Coomassie brilliant blue staining (not shown).

in the TX-100 extractable fractions (Fig. 4A, upper panel, B). Although MC-LR initially induced a small increase in the phosphorylation levels of insoluble K8 and K18, this phosphorylation was soon stabilized and the additionally phosphorylated keratin subunits appeared to be recruited into the soluble fraction (Fig. 4A). Taken together, these results indicated that a significant amount of the keratin polymer is undergoing a phosphorylation-dependent disassembly in the presence of MC-LR.

Immunoprecipitation with desmoplakin antibodies showed increased phosphorylation of DPI (250 kDa) and DPII (215 kDa) in cells incubated in the presence of MC-LR compared to control cells (Fig. 4C). Treatment with 10 µM MC-LR for 50 minutes induced an increase in the DPI/II phosphorylation levels by ×5.8 and ×4.5, respectively (Fig. 4C). The level of phosphorylation was, however, considered low compared to the induced keratin hyperphosphorylation. In Fig. 4C the DPI/II hyperphosphorylations induced by 10 µM MC-LR for 50 minutes are presented. Increases of both DPI and DPII phosphorylation could, however, be observed already at 15 minutes treatment with 4 µM MC-LR (results not shown).

The TX-100 soluble fractions were subjected to 2-D gel electrophoretic separation in order to determine whether there were any differences between the keratin isoforms in control and MC-LR-treated cells (Fig. 5A-D). Autoradiograms of 2-D gels showed that MC-LR increased the number of phosphorylated K8 and K18 isoforms. At higher MC-LR concentrations (Fig. 5C,D) two additional hyperphosphorylated forms of K8, with more acidic isoelectric points were seen. The 2-D separation also confirmed the dominant role of K8 and K18 as the major hyperphosphorylated proteins.

Fig. 5. Analysis of TX-100 soluble phosphoproteins by 2-D gel electrophoresis showing an MC-LR-induced increase in the amount of phosphorylated keratin isoforms. Autoradiographs show TX-100 soluble proteins from ^{32}P-labeled rat hepatocyte primary cultures after 2-D gel electrophoretic separation. The panel shows proteins from control cells (A) and cell treated with 4 µM MC-LR for 15 minutes (B), 30 minutes (C) and 10 µM MC-LR 50 minutes (D). Location of K8, K18 and electrophoresis directions are as indicated. x indicates an unidentified protein of molecular mass slightly smaller than K18.

In addition to keratins, several low molecular mass proteins (20-35 kDa) displayed pronounced increases in phosphorylation in the presence of MC-LR (Fig. 4A). Some of these proteins were, interestingly, co-immunoprecipitated with K8/K18 antibodies (Fig. 4B). They were, however, not detected on K8/K18 immunoblots (results not shown) indicating that they probably were not derived by proteolytic cleavage of the keratins. The phosphorylation of myosin light chain (molecular mass 20 kDa) is known to affect the assembly of MFs (Fernandez et al., 1990). As myosin light chain phosphorylation is regulated by PP1 (Fernandez et al., 1990), we tested whether PP1/PP2A inhibition by MC-LR would lead to increased phosphorylation of myosin light chain. Our results, based on immunoprecipitation and blotting, indicated that myosin light chain was not phosphorylated during MC-LR treatment (results not shown).

Evidence for assembly state-specific phosphorylation sites on K18

Phosphopeptide mapping of TX-100 soluble and insoluble keratins after MC-LR treatment revealed that certain sites in the soluble pool of K18 (denoted 1 and 5-7, Fig. 6C,D) showed significantly elevated phosphorylation (2- to 9-fold, Fig. 6E) compared to corresponding sites in the insoluble pool. The increase in labeling was highest (9.2×; Fig. 6E) for the relatively uncharged peptide numbered 1 (Fig. 6D). In contrast, there were no indications of such assembly state-specific sites on K8 as relative labeling of soluble vs insoluble keratins between the phosphopeptides were similar (Fig. 6A,B). Instead, all identified phosphopeptides showed increased labeling in both pools of K18. The specific labeling of the respective peptides seen on peptide maps in Fig. 6 reflects actual differences between soluble and insoluble protein, as equal parts of both fractions were used to generate the maps. The overall higher specific labeling of peptides derived from soluble protein (both K8 and K18) compared to peptides generated from insoluble protein, confirms the data (Fig. 4A,D) showing that most of the hyperphosphorylated keratins are disassembled.

Assessment of PKA and CaMK as possible K8 and K18 kinases in vivo

The MC-LR-induced phosphorylation was further studied by 2-D tryptic phosphopeptide mapping of keratins immunoprecipitated from whole cell extracts obtained from ^{32}P-labeled cells (Figs 7, 8). Using phosphoamino acid analysis the hyperphosphorylation on both rat liver keratins was shown to be serine-specific (results not shown). The tryptic in vivo maps were compared with maps of K8/K18 phosphorylated in vitro using CaMK or PKA, in order to elucidate the roles of these kinases in the observed effects on keratin organization and assembly. The two kinases were chosen as it is well established that they can efficiently phosphorylate type III IF proteins in vitro (Tsujimura et al., 1994; Tao and Ip, 1991) and liver keratins (Yano et al., 1991; Ando et al., 1996). There is also evidence to indicate that they are involved in interphase-specific in vivo phosphorylation of type III IF proteins (Eriksson and Goldman, 1993; J. E. Eriksson, and R. D. Goldman, unpublished results).

As shown in Fig. 7A, K8 was weakly but constitutively phosphorylated on two major tryptic peptides (2 and 4) in
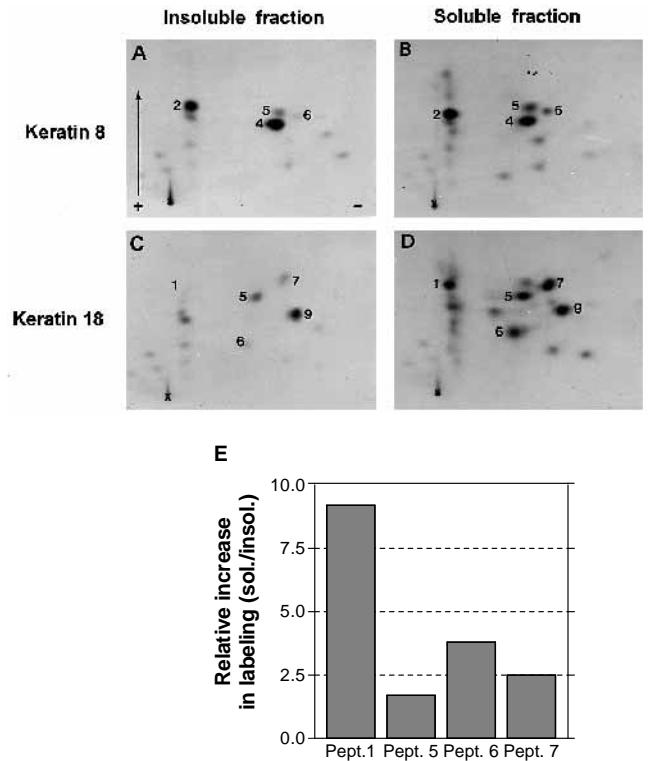

Fig. 6. Demonstration of assembly-state specific phosphorylation sites on K18. Autoradiographs of tryptic phosphopeptide maps show K8 (A and B) and K18 (C and D) from TX-100 extraction-resistant pellets (insoluble fraction; A and C) and TX-100-soluble supernatants (soluble fraction; B and D) derived from rat hepatocyte primary cultures treated with 10 μM MC-LR for 50 minutes. Direction of electrophoresis (+ and -) and ascending chromatography (arrow) are indicated. Intensities of radiolabel in figures reflect actual differences between soluble and insoluble fractions, as equal parts of both fractions were used to generate the peptide maps. Same peptides are indicated with corresponding numbers and x indicates sample loadings. Quantification of the increased labeling of K18 tryptic peptides in the soluble fraction (from C to D) is shown in E. As peptide # 9 did not show any obviously increased labeling in the soluble K18-fraction, the labeling intensities of peptide # 9 in the soluble and insoluble fractions were equalized, and the labeling intensities of peptides # 1, 5, 6, 7 are expressed as values relative to the labeling of peptide # 9. The increases in labeling of the peptides in the soluble fractions were calculated using phosphorimage analysis of the tryptic peptide maps shown on the autoradiographs in C and D. Numbering of peptides is the same as in Figs 7 and 8.

control cells. The MC-LR-induced increase in K8 phosphorylation in vivo occurred primarily on the peptides denoted 2-5 (Fig. 7B). PKA phosphorylated K8 on several peptides (Fig. 7C), two of which (peptides 4 and 5) were induced in vivo (Fig. 7B-D). However, peptide 4 was poorly labeled by PKA in vitro, suggesting that PKA might not play a dominant role in regulating the phosphorylation of this site in vivo. The CaMK-specific K8 phosphopeptide pattern corresponded well to that generated from K8 phosphorylated in vivo in the presence of MC-LR (Fig. 7E). Also the specific labeling ratios between major in vivo peptides (peptides 3-6) corresponded well to those measured on phosphopeptide maps obtained with CaMK in vitro. Our results suggest CaMK, and less likely PKA, as potential kinases regulating K8 in vivo.
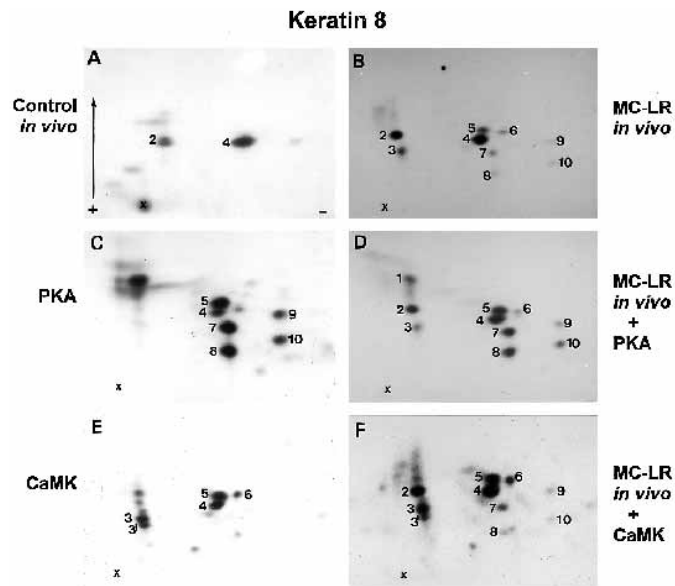
Fig. 7. Phosphopeptide mapping of possible in vivo CaMK and PKA sites on K8. Comparison of autoradiographs of tryptic phosphopeptide maps showing in vivo and in vitro phosphorylated K8. Phosphopeptide maps were derived from K8 phosphorylated in vivo in the presence of MC-LR and in vitro using either PKA or CaMK. MC-LR-in vivo maps were derived from immunoprecipitated K8 from cells incubated in the presence of 10 μM MC-LR for 50 minutes. Prior to peptide mapping, labeled keratins were separated on SDS-PAGE, cut out and digested with trypsin. Corresponding phosphopetides are denoted with the same numbers and x indicates sample loadings. Direction of electrophoresis (+ and -) and ascending chromatography (arrow) are indicated.

As shown in Fig. 8A, K18 was weakly but constitutively phosphorylated on a few tryptic peptides in control cells. The MC-LR-induced increase in phosphorylation occurred on several additional peptides (Fig. 8B), reflecting the high K18 phosphorylation seen on autoradiographs of SDS-PAGE analysis (Fig. 4B). K18 phosphorylated by PKA in vitro generated one main peptide (peptide 8, Fig. 8C) which could not be found among the major MC-LR-inducible phosphopeptides (Fig. 8B,D). Although CaMK-specific in vitro phosphorylation could be observed on 5-6 K18 peptides, the CaMK peptide map-pattern (Fig. 8E) was significantly different from that of K18 phosphorylated in vivo (Fig. 8B,F). The MC-LR-induced hyperphosphorylation of peptide 5, however, displayed rather variable levels between different in vivo experiments, presumably depending on small variations in the experimental conditions. On the peptide maps shown in Fig. 8B, peptide 5, which contains one of the major CaMK sites (Fig. 8C), was not readily induced by MC-LR, while in other identical experiments (see Fig. 6C-D) it constituted one of the major in vivo sites. Immunoprecipitated K8 and K18 from MC-LR-treated hepatocytes in suspension culture showed phosphopeptide maps very similar (data not shown) to those generated from material isolated from cultures grown in Petri dishes. This indicates that the major phosphorylation sites on K8/K18 are not induced by the growth conditions used for these experiments.
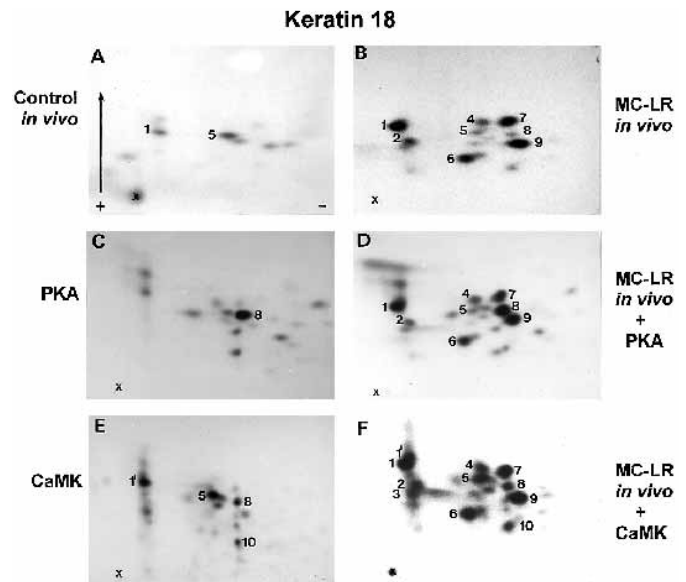

Fig. 8. Phosphopeptide mapping of possible in vivo CaMK and PKA sites on K18. Comparison of autoradiographs showing tryptic phosphopeptide maps of in vivo and in vitro phosphorylated K18. The panel shows in vivo and in vitro phosphorylated K18 as indicated. Conditions and labels are as in Fig. 7.

DISCUSSION

The results of this study clearly demonstrate that constitutive protein phosphatase activities are required to maintain both normal cellular interactions and cytoskeletal structure. This conclusion is based upon our findings which show that down-regulation of ser/thr protein phosphatase activities with MC-LR disrupts cell junctions and the organization of IFs and MFs. The most pronounced effects of protein phosphatase inhibition involved reorganization and disassembly of keratin IFs due to hyperphosphorylation of the normally stable filament polymers. By detailed analysis of the sequence of these effects, we have been able to elucidate a number of phosphorylation-dependent regulatory mechanisms relating to keratin IFs, including control of assembly, interactions with desmosomes, and association with MFs.

Phosphorylation-dependent interaction of keratin IFs with desmosomes

The first obvious effects in primary cultures of rat hepatocytes exposed to MC-LR were observed on desmosomes as an altered organization of desmoplakin, followed by an immediate withdrawal of keratin IFs from the same locations at the cell surface. Desmoplakin is involved in the IF-desmosome association (Miller et al., 1987; Jones and Grelling, 1989; Garrod, 1993; Kouklis et al., 1994), which appears to be mediated by the C-terminal domain of desmoplakin (Stappenbeck et al., 1994). Also the IFAP 300 protein has been suggested to be involved in this IF-desmosome contact (Skalli et al., 1994). The decline in desmoplakin-immunostaining that we observed, occurred in concert with increased phosphorylation of DPI/II. A previous study suggests that the phosphorylation of ser-23 on desmoplakin may negatively regulate its interaction with

keratin filaments (Stappenbeck et al., 1994). Our observations, that are in agreement with a recent study on cell junctions in epithelial cells treated with okadaic acid (Pasdar et al., 1995), could thus be explained by this type of negative regulation. According to this scheme, impaired dephosphorylation of DPI/II, leads to the loosening of cell junctions which is associated with the loss of contacts to cytoplasmic IFs. Interestingly, phosphatase inhibition also seemed to induce an increased disassembly of desmoplakin, as demonstrated by elevated diffuse desmoplakin immunoreactivity. This suggests that not only the desmoplakin-IF interactions are regulated by phosphorylation but, possibly, also the assembly state of these desmosomal proteins. Our results also help to explain the previously observed loss of desmosomes in liver from rats injected with MC-LR (Miura et al., 1989).

Phosphorylation-induced reorganization and disassembly of keratin polymers

Along with the effects observed on desmosomes, MC-LR also induced a marked morphological reorganization and disassembly of keratin IFs. This sequence of effects correlated well with an increased phosphorylation of K8 and K18, that were among the principal hyperphosphorylated MC-LR-induced phosphoproteins. Our findings are in agreement with the rather well established paradigm stating that the organization and assembly states of IFs are regulated by phosphorylation of their constitutive proteins. Increased phosphorylation of a number of IF proteins have been shown to cause disassembly or prevent subunit polymerization both in vitro and in vivo (reviewed by Eriksson et al., 1992b; Nigg, 1992; Eriksson and Goldman, 1993). In agreement with this principle, K8 and K18 normally show relatively low levels of phosphorylation and the bulk of these proteins exist in the polymerized state.

Our results imply that the steady-state regulation of K8/K18 in hepatocytes involves a phosphorylation-dephosphorylation cycle as the K8/K18 filament structure, as well as polymer stability, are immediately disrupted upon phosphatase inhibition. This is supported by our data showing that K8 and K18 are solubilized in TX-100 in concert with their hyperphosphorylation. Analogously, it has been shown that ser/thr-specific phosphatase inhibition induces hyperphosphorylation and disassembly of the type III IF protein vimentin (Eriksson et al., 1992a; Eriksson and Goldman, 1993; Almazan et al., 1993), the type IV IFs, the neurofilament triplet proteins (Sacher et al., 1992, 1994) and the type VI IF protein nestin (Almazan et al., 1993). Taken together these observations indicate that the inhibition of the major IF phosphatase activities, constituted by PP1 and/or PP2A, generally leads to IF hyperphosphorylation and disassembly. Based on the present work, we can conclude that the ser/thr protein phosphatases, PP1 and/or PP2A, are very important regulators of K8 and K18 IF organization and stability. The specific roles of PP1 vs PP2A in regulation of IF proteins are still not established. However, preliminary results obtained with vimentin, indicate that they have different site-specificities (J. E. Eriksson and R. D. Goldman, unpublished results).

CaMK and PKA as potential counterparts to PP1/PP2A in the regulation of K8 and K18 phosphorylation

It is obvious from this and several other studies that PP1 and PP2A are the main regulators of IF protein (de)phosphorylation. Surprisingly little is, however, known about their in vivo IF kinase counterparts, especially those involved in keratin phosphorylation. In vitro it has been shown that keratins can be phosphorylated by several kinases such as CaMK, S6-kinase, PKCε (Ku and Omary, 1994) and PKA (Ando et al., 1996). Our study provides evidence to suggest a role for one of these kinases in vivo. Based on our comparative in vivo/in vitro peptide mapping, we suggest that CaMK may have a possible role in regulating K8 phosphorylation in hepatocytes. Although PKA peptide maps also showed some resemblance with those obtained from in vivo phosphorylated K8, the low labeling on the PKA-specific peptides in vivo, however, indicated that PKA may not play a major role in the interphase-specific regulation of K8. Previous studies have indicated that PKA and CaMK are involved in the interphase regulation of at least type III IF proteins (Eriksson and Goldman, 1993; J. E. Eriksson and R. D. Goldman, unpublished observations).

The in vivo phosphorylation pattern of K18 is rather complex. Based on our comparative peptide mapping results, PKA is not likely to play a role in the regulation of K18. CaMK seems to act on one of the in vivo-inducible sites (Fig. 8, peptide denoted 5). However, the MC-LR-induced in vivo phosphorylation of peptide 5 in vivo varies, based on the finding that different degrees of phosphorylation were obtained in different experiments. As this is a major CaMK peptide in vitro, the variation in vivo could reflect variations in intracellular Ca^{2+}-specific signaling during different experiments. Hence, CaMK may to some extent contribute to the phosphorylation of K18 in vivo, although more detailed studies are required to confirm its action. Interestingly, ser-52, a major phosphorylation site on human K18 (Ku and Omary, 1994), is situated in a consensus sequence of CaMK. This site, the roles of which appears to be associated with filament disassembly (Ku and Omary, 1994), could, hence, be regulated by CaMK. However, as most of the major K18 inducible phosphopeptides described in our study are neither CaMK nor PKA sites, the action of some other kinase(s) must be important in regulation of K18 phosphorylation.

We have also attempted to detect phosphorylation sites that could be specific for disassembled keratins. The MC-LR-induced solubility/disassembly of K8 appears to be due to increased phosphorylation on all tryptic phosphopeptides. In contrast, K18 showed that four, out of five, main tryptic peptides were highly phosphorylated in the soluble fraction, compared to the insoluble fraction. As phosphorylation on these four sites seem to favor disassembly of keratins, they are likely to be important in regulating the assembly-states of keratin filaments. Taken together, this is the first evidence to show that there are specific disassembly-promoting in vivo phosphorylation sites on K18. It is obvious that, although K8 and K18 form heterodimers that are basic structural units of keratin IFs, their phosphorylation patterns are surprisingly different. Our study as well as a previous study (Liao et al., 1995) show that K8 has a higher degree of constitutive phosphorylation than K18. Furthermore, K8 does not show such marked increases in phosphorylation upon inhibition of dephosphorylation as K18. These results imply that a significant proportion of the constitutive phosphorylation of keratin polymers resides on K8 whereas most of the IF-specific phosphate turnover occurs on K18.

Manifestation of an uncharacterized association between MFs and IFs

We observed a simultaneous reorganization of MFs with the keratin IFs as they merged into one filamentous structure. This result implies an intriguing, but poorly studied, association between these two major cytoskeletal components. There is some evidence to show that IFs might be associated with MFs (Green et al., 1986, 1987; Tint et al., 1991), i.e. in livers around the bile canaliculi (reviewed by van Eyken and Desmet, 1993). Our study implies that the nature of the IF/MF association is rather firm as it still could be seen after prolonged incubation in the presence of MC-LR. The MF-associated IFs also seemed to be more resistant to phosphorylation-induced disassembly, as obvious filamentous IF structures could be observed in the region of the IF-MF bundle, while the bulk of the keratin IFs in the rest of the cell had disassembled. Indications of a similar association between vimentin IFs and MFs were shown in fibroblasts treated with calyculin A (Hirano et al., 1992). The MF-IF complex could be isolated together with the nuclear fraction, indicating that vimentin must have been attached both to the nucleus and to the MFs. This co-reorganization is more likely to be driven by forces acting on the MFs rather than IFs. There is significant evidence to show that actin organization is partly dependent on the phosphorylation state of myosin light chain (Lamb et al., 1988; Fernandez et al., 1990). We did not, however, observe any increased phosphorylation of myosin light chain, which is in agreement with earlier observations on calyculin A-treated fibroblast (Eriksson et al., 1992a) and thrombocytes (Yano et al., 1995). It is also known that the MC-LR-induced reorganization is not due to a shift in G/F-actin ratios (Eriksson et al., 1989). The appearance of the phosphatase inhibitor-induced actin complex does not seem to be due to phosphorylation of actin itself (Eriksson and Goldman, 1993). Involvement of some of the phosphorylation-dependent actin-associated proteins might be important in this context.

The cellular basis of microcystin-induced organ damage

Our results help to provide a rational interpretation of the severe organ-disrupting effect demonstrated in many previous studies to be characteristic for the action of microcystins (Falconer et al., 1981; Eriksson et al., 1988; Hooser et al., 1989). In the parenchymal liver cells, the loss of desmosomal integrity together with the morphological and cytoskeletal alterations, will strongly impair hepatocyte attachment and cause cellular dissociation. Perturbation of IF-desmosome contacts has been shown to result in loss of tissue integrity (Stanley, 1993). The cytoskeleton-based alterations in cellular morphology and the detachment of parenchymal cells in combination with the hydrostatic pressure in the sinusoids will be sufficient to reduce vascular integrity and cause severe hemorrhages in the liver tissue, as previously suggested (Eriksson and Goldman, 1993; Carmichael, 1994). The effects on keratin IFs and their inter-actions with other cytoskeletal elements is especially pro-nounced as both reorganization and disassembly of the con-stituent polymers can be seen. In support of this is an earlier study on the effects of MC-LR on rat liver showing a loss of keratins from the detergent extraction-resistant fraction (Miura et al., 1989). In summary, we demonstrate that there is a require-ment for constitutive protein phosphatase activities in the main-tenance of the structural integrity of both cells and tissues.

REFERENCES

Almazan, G., Afar, D. E. H. and Bell, J. C. (1993). Phosphorylation and disruption of intermediate filament proteins in oligodendrocyte precursor cultures treated with calyculin A. *J. Neurosci. Res.* **36**, 163-172.

Ando, S., Tokui, T., Yano, T. and Inagaki, M. (1996). Keratin 8 phosphorylation in vitro by cAMP-dependent protein kinase occurs within the amino- and carboxy-terminal end domains. *Biochem. Biophys. Res. Commun.* **221**, 67-71.

Carmichael, W. W. (1994). The toxins of cyanobacteria. *Sci. Am.* **270**, 64-72.

Cowin, P. and Garrod, D. R. (1983). Antibodies to epithelial desmosomes show wide tissue and species cross-reactivity. *Nature* **302**, 148-150.

Deery, W. J. (1993). Role of phosphorylation in keratin and vimentin filament integrity in cultured thyroid epithelial cells. *Cell Motil. Cytoskel.* **26**, 325-339.

Downey, G. P., Takai, A., Zamel, R., Grinstein, S. and Chan, C. K. (1993). Okadaic acid-induced actin assembly in neutrophils: Role of protein phosphatases. *J. Cell. Physiol.* **155**, 505-519.

Eriksson, J. E., Meriluoto, J. A. O., Kujari, H. P., Österlund, K., Fagerlund, K. and Hällbom, L. (1988). Preliminary characterization of a toxin isolated from the cyanobacterium *Nodularia spumigena*. *Toxicon* **26**, 161-166.

Eriksson, J. E., Paatero, G. I. L., Meriluoto, J. A. O., Codd, G. A., Kass, G. E. N., Nicotera, P. and Orrenius, S. (1989). Rapid microfilament reorganization induced in isolated rat hepatocytes by microcystin-LR, a cyclic peptide toxin. *Exp. Cell Res.* **185**, 86-100.

Eriksson, J. E., Toivola, D., Meriluoto, J. A. O., Karaki, H., Han, Y.-G. and Hartshorne, D. (1990a). Hepatocyte deformation induced by cyanobacterial toxins reflects inhibition of protein phosphatases. *Biochem. Biophys. Res. Commun.* **173**, 1347-1353.

Eriksson, J. E., Grönberg, L., Nygård, S., Slotte, J. P. and Meriluoto, J. A. O. (1990b). Hepatocellular uptake of ³H-dihydromicrocystin-LR, a cyclic peptide toxin. *Biochim. Biophys. Acta* **1025**, 60-66.

Eriksson, J. E., Brautigan, D. L., Vallee, R. D., Olmsted, J., Fujiki, H. and Goldman, R. D. (1992a). Cytoskeletal integrity in interphase cells requires protein phosphatase activity. *Proc. Nat. Acad. Sci. USA* **89**, 11093-11097.

Eriksson, J. E., Opal, P. and Goldman, R. D. (1992b). Intermediate filament dynamics. *Curr. Opin. Cell Biol.* **4**, 99-104.

Eriksson, J. E. and Goldman, R. D. (1993). Protein phosphatase inhibitors alter cytoskeletal structure and cellular morphology. *Advan. Prot. Phosph.* **7**, 335-357.

Falconer, I. R., Jackson, A. R. B., Langely, J. and Runnegar, M. T. (1981). Liver pathology in mice in poisoning by the blue-green algae *Microcystis aeruginosa*. *Aust. J. Biol. Sci.* **34**, 179-187.

Falconer, I. R. and Yeung, D. S. K. (1992). Cytoskeletal changes in hepatocytes induced by *Microcystis* toxins and their relation to hyperphosphorylation of cell proteins. *Chem.-Biol. Interact.* **81**, 181-196.

Fernandez, A., Brautigan, D. L., Mumby, M. and Lamb, N. J. C. (1990). Protein phosphatase type-1, not type-2A, modulates actin microfilament integrity and myosin light chain phosphorylation in living nonmuscle cells. *J. Cell Biol.* **111**, 103-112.

Fujiki, H. and Suganuma, M. (1993). Tumor promotion by inhibitors of protein phosphatases 1 and 2A: The okadaic acid class of compounds. *Advan. Cancer Res.* **61**, 143-194.

Garrod, D. R. (1993). Desmosomes and hemidesmosomes. *Curr. Opin. Cell Biol.* **5**, 30-40.

Green, K. J., Talian, J. C. and Goldman, R. D. (1986). Relationship between intermediate filaments and microfilaments in cultured fibroblasts: Evidence for common foci during cell spreading. *Cell Motil. Cytoskel.* **6**, 406-418.

Green, K. J., Geiger, B., Jones, J. C. R., Talian, J. C. and Goldman, R. D. (1987). The relationship between intermediate filaments and microfilaments before and during the formation of desmosomes and adherens type junctions in mouse epidermal keratinocytes. *J. Cell Biol.* **104**, 1389-1402.

Heins, S. and Aebi, U. (1994). Making heads and tails of intermediate filament assembly, dynamics and networks. *Curr. Opin. Cell Biol.* **6**, 25-33.

Hirano, K., Chartier, L., Taylor, R. G., Allen, R. E., Fusetani, N., Karaki, H. and Hartshorne, D. J. (1992). Changes in the cytoskeleton of 3T3 fibroblasts induced by the phosphatase inhibitor, calyculin A. *J. Muscle Res. Cell Motil.* **13**, 341-353.

Holmes, C. F. B and Boland, M. P. (1993). Inhibitors of protein phosphatase-1 and-2A; two of the major serine/threonine protein phosphatases involved in cellular regulation. *Curr. Opin. Struct. Biol.* **3**, 934-943.

Hooser, S. B., Beasley, V. R., Lovell, R. A., Carmichael, W. W. and Hascheck, W. M. (1989). Toxicity of microcystin-LR, a cyclic heptapeptide hepatotoxin from *Microcystis aeruginosa*, to rats and mice. *Vet. Pathol.* **26**, 246-252.

Hosoya, N., Mitsui, M., Yazama, F., Ishihara, H., Ozaki, H., Karaki, H., Hartshorne, D. J. and Mohri, H. (1993). Changes in the cytoskeletal structure of cultured smooth muscle cells induced by calyculin A. *J. Cell Sci.* **105**, 883-890.

Jones, J. C. and Grelling, K. A. (1989). Distribution of desmoplakin in normal cultured human keratinocytes and in basal cell carcinoma cells. *Cell Motil. Cytoskel.* **13**, 181-194.

Kasahara, K., Kartasova, T., Ren, X.-q., Ikuta, T., Chida, K. and Kuroki, T. (1993). Hyperphosphorylation of keratins by treatment of okadaic acid of BALB/MK-2 mouse keratinocytes. *J. Biol. Chem.* **268**, 23531-23537.

Kouklis, P. D., Hutton, E. and Fuchs, E. (1994). Making a connection: Direct binding between keratin intermediate filaments and desmosomal proteins. *J. Cell Biol.* **127**, 1049-1060.

Kreinbühl, P., Keller, H. and Niggli, V. (1992). Protein phosphatase inhibitors okadaic acid and calyculin A alter cell shape and F-actin distribution and inhibit stimulus-dependent increases in cytoskeletal actin of human neutrophils. *Blood* **80**, 2911-2919.

Ku, N.-O. and Omary, M. B. (1994). Identification of the major physiologic phosphorylation site of human keratin 18: Potential kinases and a role in filament reorganization. *J. Cell Biol.* **127**, 161-171.

Kurisaki, T., Magae, J., Nagai, K., Hirata, A., Kusaka, I., Shinji, H., Morikawa, M., Yoshida, T., Isono, K. and Yamasaki, M. (1993). Morphological changes and reorganization of actin filaments in human myeloid leukemia cells induced by a novel protein phosphatase inhibitor, tautomyocin. *Cell. Struct. Funct.* **18**, 33-39.

Laemmli, U. K. (1970). Cleavage of structural proteins during the assembly of the head of bacteriophage T4. *Nature* **227**, 680-685.

Lamb, N. J. C., Fernandez, A., Conti, M. A., Adelstein, R., Glass, D. B., Welch, W. J. and Feramisco, J. R. (1988). Regulation of actin microfilament integrity in living nonmuscle cells by the cAMP-dependent protein kinase and the myosin light chain kinase. *J. Cell Biol.* **106**, 1955-1971.

Lee, W.-C., Yu, J.-S., Yang, S.-D. and Lai, Y.-K. (1992). Reversible hyperphosphorylation and reorganization of vimentin intermediate filaments by okadaic acid in 9L brain tumor cells. *J. Cell. Biochem.* **49**, 378-393.

Liao, J., Lowthert, L. A., Ku, N.-O., Fernandez, R. and Omary, M. B. (1995). Dynamics of human keratin 18 phosphorylation: polarized distribution of phosphorylated keratins in simple epithelial tissues. *J. Cell Biol.* **131**, 1291-1301.

MacKintosh, R. W., Dalby, K. N., Campbell, D. G., Cohen, P. T. W., Cohen, P. and MacKintosh, C. (1995). The cyanobacterial toxin microcystin binds covalently to cystein-273 on protein phosphatase 1. *FEBS Lett.* **371**, 236-240.

Maier, G. D., Wright, M. A., Lozano, Y., Djordjevic, A., Matthews, J. P. and Young, M. R. I. (1995). Regulation of cytoskeletal organization in tumor cells by protein phosphatases-1 and –2A. *Int. J. Cancer* **61**, 54-61.

Meriluoto, J. A. O. and Eriksson, J. E. (1988). Rapid analysis of peptide toxins in cyanobacteria. *J. Chromatogr.* **438**, 93-99.

Meriluoto, J. A. O., Nygård, S. E., Dahlem, A. M. and Eriksson, J. E. (1990). Synthesis, organotropism and hepatocellular uptake of two tritium-labelled epimers of dihydromicrocystin-LR, a cyanobacterial peptide toxin analog. *Toxicon* **28**, 1439-1446.

Miller, K., Mattey, D., Measures, H., Hopkins, C. and Garrod, D. (1987). Localisation of the protein and glycoprotein components of bovine nasal epithelial desmosomes by immunoelectron microscopy. *EMBO J.* **6**, 885-889.

Miura G. A., Robinson, N. A., Geisbert, T. W., Bostian, K. A., White, J. D. and Pace, J. G. (1989). Comparison of in vivo and in vitro toxic effects of microcystin-LR in fasted rats. *Toxicon* **27**, 1229-1240.

Nigg, E. A. (1992). Assembly-disassembly of the nuclear lamina. *Curr. Opin. Cell Biol.* **4**, 105-109.

O'Farrell, P. H. (1975). High resolution two-dimensional electrophoresis of proteins. *J. Biol. Chem.* **250**, 4007-4021.

Ohta, T., Nishiwaki, R., Yatsunami, J., Komori, A., Suganuma, M. and Fujiki, H. (1992). Hyperphosphorylation of cytokeratins 8 and 18 by microcystin-LR, a new liver tumor promoter, in primary cultured rat hepatocytes. *Carcinogensis* **13**, 2443-2447.

Ottaviano, Y. and Gerace, L. (1985). Phosphorylation of the nuclear lamins during interphase and mitosis. *J. Biol. Chem.* **260**, 624-632.

Parrish, E. P., Steart, P. V., Garrod, D. R. and Weller, R. O. (1987). Antidesmosomal monoclonal antibody in the diagnosis of intracranial tumors. *J. Pathol.* **153**, 265-273.

Pasdar, M., Li, Z. and Chan, H. (1995). Desmosome assembly and disassembly are regulated by reversible protein phosphorylation in cultured epithelial cells. *Cell Motil. Cytoskel.* **30**, 108-121

Runnegar, M. T. C. and Falconer, I. R. (1986). Effects of toxin from the cyanobacterium *Microcystis aeruginosa* on ultrastrucutral morphology and actin polymerization in isolated hepatocytes. *Toxicon* **24**, 109-115.

Runnegar, M. T. C., Gerdes, R. G. and Falconer, I. R. (1991). The uptake of the cyanobacterial hepatotoxin microcystin by isolated rat hepatocytes. *Toxicon* **29**, 43-51.

Sacher, M. G., Athlan, E. S. and Mushynski, W. E. (1992). Okadaic acid induces the rapid and reversible disruption of the neurofilament network in rat dorsal root ganglion neurons. *Biochem. Biophys. Res. Commun.* **186**, 524-530.

Sacher, M. G., Athlan, E. S. and Mushynski, W. E. (1994). Increased phosphorylation of the amino-terminal domain of the low molecular weight neurofilament subunit in okadaic acid-treated neurons. *J. Biol. Chem.* **269**, 18480-18484.

Seglen, P. O. (1976). Preparation of isolated rat liver cells. *Meth. Cell Biol.* **13**, 71-98.

Skalli, O., Jones, J. C., Gagescu, R. and Goldman, R. D. (1994). IFAP 300 is common to desmosomes and hemidesmosomes and is a possible linker of intermediate filaments to these junctions. *J. Cell Biol.* **125**, 159-170.

Stanley, J. R. (1993). Cell adhesion molecules as targets of auto antibodies in pemphigus and pemphigoid bullos diseases due to defective epidermal cell adhesion. *Advan. Immunol.* **53**, 291-325.

Stappenbeck, T. S., Lamb, J. A., Corcoran, C. M. and Green, K. J. (1994). Phosphorylation of the desmoplakin COOH terminus negatively regulates its interaction with keratin intermediate filament networks. *J. Biol. Chem.* **269**, 29351-29354.

Tao, J. X. and Ip, W. (1991). Site-specific antibodies block kinase A phosphorylation of desmin in vitro and inhibit incorporation of myoblasts into myotubes. *Cell Motil. Cytoskel.* **19**, 109-120.

Tint, I. S., Hollenbeck, P. J., Verkhovsky, A. B., Surgucheva, I. G. and Bershadsky, A. D. (1991). Evidence that intermediate filament reorganization is induced by ATP-dependent contraction of the actomyosin cortex in permeabilized fibroblasts. *J. Cell Sci.* **98**, 375-384.

Toivola, D. M., Eriksson, J. E. and Brautigan, D. L. (1994). Identification of protein phosphatase 2A as the primary target for microcystin-LR in rat liver homogenates. *FEBS Lett.* **344**, 175-180.

Tsujimura, K., Tanaka, J., Ando, S., Matsuoka, Y., Kusubata, M., Sugiura, H., Yamauchi, T. and Inagaki, M. (1994). Identification of phosphorylation sites on glial fibrillary acidic protein for cdc2 kinase and Ca^{2+}-calmodulin-dependent protein kinase II. *J. Biochem. (Tokyo)* **116**, 426-434.

van der Geer, P., Luo, K., Sefton, B. M. and Hunter, T. (1993). Phosphopeptide mapping and phosphoamino acid analysis on cellulose thin-layer plates. In *Protein phosphorylation, A Practical Approach* (ed. D. G. Hardie), pp. 31-59. IRL Press, Oxford University Press, New York.

van Eyken, P. and Desmet, V. J. (1993). Cytokeratins and the liver. *Liver* **13**, 113-122.

Wickstrom, M. L., Khan, S. A., Haschek, W. M., Wyman, J. F., Eriksson, J. E., Schaeffer, D. J. and Beasley, V. R. (1995). Alterations in microtubules, intermediate filaments, and microfilaments induced by microcystin-LR in cultured cells. *Toxicol. Pathol.* **23**, 326-337.

Yano, T., Tokui, T., Nishi, Y., Nishizawa, K., Shibata, M., Kikuchi, K., Tsuiki, S., Yamauchi, T. and Inagaki, M. (1991). Phosphorylation of keratin intermediate filaments by protein kinase C, by calmodulin-dependent kinase and by cAMP-dependent kinase. *Eur. J. Biochem.* **197**, 281-290.

Yano, Y., Sakon, M., Kambayashi, J.-i., Kawasaki, T., Senda, T., Tanaka, K., Yamada, F. and Shibata, N. (1995). Cytoskeletal reorganization of human platelets induced by the protein phosphatase 1/2A inhibitors okadaic acid and calyculin A. *Biochem. J.* **307**, 439-449.